Title

Identifying geochemical hot moments and their controls on a contaminated river floodplain system using wavelet and entropy approaches

Authors

Arora, B
Dwivedi, D
Hubbard, SS
et al.

Publication Date

2016-11-01

DOI

10.1016/j.envsoft.2016.08.005

Peer reviewed

Identifying geochemical hot moments and their controls on a contaminated river floodplain system using wavelet and entropy approaches

Bhavna Arora*, Dipankar Dwivedi, Susan S. Hubbard, Carl I. Steefel, Kenneth H. Williams

Lawrence Berkeley National Laboratory, United States

* Corresponding author. Energy Geosciences Division, Lawrence Berkeley National Laboratory, 1 Cyclotron Rd., MS 74-327R, Berkeley, CA, 94720, United States. E-mail address: barora@lbl.gov (B. Arora).

Abstract

Geochemical hot moments are defined here as short periods of time that are associated with disproportionally high levels of concentrations (biogeochemically-driven or transport-related) relative to longer intervening time periods. We used entropy and wavelet techniques to identify temporal variability in geochemical constituents and their controls along three transects within a contaminated floodplain system near Rifle CO. Results indicated that transport-dominated hot moments drove overall geochemical processing in the contaminated groundwater and seep zones. These hot moments were associated with seasonal hydrologic variability (~4 months) in the contaminated aquifer and with annual hydrologic cycle and residence times in the seep zone. Hot moments associated with a naturally reduced zone within the aquifer were found to be biogeochemically-driven, with a different dominant frequency (~3 months) and no correlation to hydrologic or weather variations, in contrast to what is observed in other regions of the floodplain.

Keywords: Wavelet analysis, Temporal variability, Biogeochemical processes, Field data

1. Introduction

Evaluating the consequences of anthropogenic activities on surface and subsurface waters and developing optimal management strategies require an understanding of the underlying hydrological, geochemical and microbiological processes that govern contaminant transport and attenuation. Developing such an understanding is challenging due to the spatial and temporal variability of hydrological and biogeochemical processes that govern transport within naturally heterogeneous terrestrial environments. In this study, we develop approaches to identify temporal variability in geochemical constituents and their controls in a complex contaminated floodplain system.

Biogeochemical processes in riverine floodplains regulate contaminant movement and often mitigate fluxes originating from upstream and upslope areas (Arora et al., 2015; Pinay et al., 2002; Schirmer et al., 2014). Several

studies have documented how hydrological perturbations, such as seasonal water table dynamics and precipitation events, influence the migration and distribution of contaminants in river systems. For example, Vazquez et al. (2010) reported changes in the characteristics and composition of dissolved organic matter in a Mediterranean fluvial system during a summer drought event. Harms and Grimm (2008) suggested that peak nitrogen retention and removal occurred during the monsoon season and coincided with seasonal shifts in microbial community carbon use in the riparian zone of the San Pedro River, Arizona. Other studies have documented the importance of rain and snowmelt events, the seasonality and direction of groundwater flow, as well as river stage fluctuations on the variability of geochemical concentrations (Arora et al., 2013; Fendorf et al., 2010; McGuire et al., 2000; Scholl et al., 2006).

These temporally non-uniform events are known to form hot moments. Hot moments are traditionally defined as short periods of time that are associated with disproportionally high levels of activity (reaction rates, concentrations, or fluxes) relative to longer intervening time periods (McClain et al., 2003). Based on the type of activity, Vidon et al. (2010) made a distinction between biogeochemical process-driven and transport-driven hot moments. As the name suggests, *biogeochemical hot moments* are defined as shortlived, high levels of *biogeochemical reaction rates* relative to longer intervening time periods. Similarly, *transport-driven hot moments* are defined as short-lived, high levels of *geochemical concentrations and/or fluxes* relative to longer intervening time periods. Both types of hot moments are relevant in a floodplain setting as they can increase or decrease the pools and fluxes of geochemical constituents and significantly impact ecosystem response. For example, Hurley et al. (1998) showed that transportdriven hot moments i.e. spring melt and storm events are important contributors of mercury loading to Lake Michigan and can significantly impact fish spawning and ecosystem health. Similarly, Palta et al. (2014) linked nitrate removal from urban storm water to biogeochemical hot moments—anaerobic conditions and nitrate availability—in brownfield wetlands. Several studies have emphasized the importance of identifying both types of geochemical hot moments to improve water quality management at floodplain and watershed scales (Lair et al., 2009; Vidon et al., 2010). Other studies have stressed the importance of including these hot moments and seasonal variations in model architecture so as to capture carbon, nutrient and contaminant fluxes in terrestrial ecosystems accurately (Frei et al., 2012; Groffman et al., 2009; Zhu et al., 2012). These studies argue that it is crucial to identify both transport-related and biogeochemically-driven hot moments and their specific controls.

In heterogeneous and temporally variable floodplain environments, biogeochemical hot moments occur as a result of a unique combination of electron donors, electron acceptors, nutrient pools and redox conditions, while transport-driven hot moments occur because of intense hydrological

events (e.g., precipitation pulses, snowmelt periods). However, the two types of hot moments are not mutually exclusive (Andrews et al., 2011; Vidon et al., 2010). The governing types of hot moments can thus be difficult to interpret because their controls can depend on either transport or biogeochemical factors, or both. For example, Andrews et al. (2011) suggested that dissolved organic carbon transport was strongly correlated with both temperature (related to biogeochemical processes) and stream discharge (linked to transport) in the Shale Hills Catchment. Liu (2013) reported that changes in redox sensitive elements were associated with both major hydrological events as well as seasonal changes in biogeochemical conditions across a range of hydrogeomorphic settings in the White River watershed, Indiana. While these and other studies have used statistical analysis or data integration methods to identify hot moments and their role in governing contaminant system behavior, lacking is a systematic approach to interrogate complex, multivariate datasets to facilitate the identification of such hot moments and their associated controls.

In this study, we used wavelet analysis to identify geochemical hot moments and Shannon entropy to identify the association of hot moments to transport and/or biogeochemical factors. Wavelet analysis is a powerful technique that can decompose the data in time and frequency domains simultaneously (Foufoula-Georgiou and Kumar, 1994; Lau and Weng, 1995). This time frequency localization property of wavelets is useful for identifying hot moments because biogeochemical datasets in contaminated river systems can show high natural variability on different time scales. Wavelet analysis is thus advantageous over classical spectral frequency methods such as Fourier transform which can only retrieve the frequencies present in the data but not the time when these frequencies occur. Recent studies have also emphasized the potential of wavelet analysis over other commonly-used statistical approaches. For example, Zhang et al. (2006) showed that simple linear regression and Mann-Kendall test reveal a decreasing trend in the upper Yangtze River and increasing trends in the middle and lower Yangtze River highlighting a flood hazard in the middle reaches. On the other hand, wavelet transform was able to present a synthesis of frequency changes and revealed that trends in stream flow were not influenced by a single factor like climatic change, but by multiple factors like destruction of vegetation and human intervention. Therefore, the main advantage of using wavelet analysis over other techniques is its ability to preserve and display information at hierarchical scales (Bradshaw and Spies, 1992; Lau and Weng, 1995; Torrence and Compo, 1998).

This wavelet-derived information at relevant time scales can be further combined with Shannon entropy methods to meaningfully characterize geochemical hot moments as transport-related or biogeochemically-driven. In information theory, Shannon entropy is regarded as a statistical measure of the number of microscopic ways that a given macroscopic state can be realized (Shannon, 1948; Singh, 2011; Starck et al., 1998). In recent years,

mutual information has been widely applied to measure the statistical dependence between variables. Mutual information is defined as the amount of information that one variable contains about the other (Dwivedi and Mohanty, 2016; Maes et al., 1997; Steuer et al., 2002). Because governing transport or biogeochemical factors can contain noisy information or have a delayed response on the evolution of geochemical hot moments, mutual information is a powerful metric that preserves system memory and quantifies the statistical dependence between systems as they evolve in time. The main advantage of using entropy over other techniques is that it is a non-parametric approach and does not make any assumptions regarding the nature of the functional dependence implicit in biogeochemical datasets (Costa et al., 2002; Singh, 1997). Several studies have emphasized the power and strengths of mutual information in comparison to other statistical techniques such as correlation analysis and similarity-based measures (Li, 1990; Pluim et al., 2003; Strehl et al., 2000).

While the application of the combined wavelet-entropy metric is not entirely new (Brunsell et al., 2008; Labat, 2005; Quiroz et al., 2011), this is the first study that explores the use of this waveletentropy combination to identify temporal variability in a multivariate geochemical dataset and relate this variability to associated transport and biogeochemical factors at distinct temporal scales.

The objectives of this study are to develop, apply and assess the value of wavelet and Shannon entropy approaches for: (1) identifying hot moments of conservative and redox sensitive species along different transects of a contaminated river floodplain, and (ii) interpreting the transport and/or biogeochemical factors controlling this temporal variability. We hypothesize that transects predisposed to flow networking (e.g., topography controlled, parallel to groundwater flow direction) will be dominated by transportdriven hot moments, while transects predisposed to flow accumulation (e.g., clay lenses in sandy aquifer) will be guided by biogeochemically-driven hot moments. We further expect that variability in geochemical constituents along transport-dominated transects will be guided by pulsed events, hydrologic fluctuations and weather controls at different time scales, while biogeochemically-driven hot moments will depend on site characteristics. Site characteristics such as spatial mineral distribution, soil structure and heterogeneous land cover can respond to varying flow regimes (e.g., low permeability interfaces, preferential flow paths) and perturbations (e.g., rainfall events, temperature fluctuations, groundwater variations) to modify aqueous geochemical conditions and reaction rates resulting in geochemical hot moments (Liu et al., 2014; Salehikhoo and Li, 2015; Sassen et al., 2012). However, biogeochemical process-driven transects may not be a dominant control of geochemical hot moments at longer time scales as the overall net processing of various geochemical constituents may be transport limited (Vidon et al., 2010). Thus, three different transects e first, parallel to the groundwater flow direction, second, along seeps, and third, a hotspot of

biogeochemical cycling - were analyzed to determine the types of geochemical hot moments within a floodplain site. We performed our study at a uranium-contaminated floodplain site near Rifle, CO.

2. Field site and datasets

2.1. Site description

The Rifle site is a former uranium and vanadium milling operations site in Rifle, Colorado located on the floodplain of the Colorado River (Fig. 1). The Rifle floodplain is approximately 750 m in length along the river shore and 250 m at the widest point (Yabusaki et al., 2011). Detailed descriptions of the site can be found elsewhere (Anderson et al., 2003; U.S. Department of Energy, 1999; Vrionis et al., 2005). Although mill tailings and contaminated sediments were removed in 1966 as part of the site cleanup efforts, several studies have documented residual uranium contamination within the local aquifer (Anderson et al., 2003; Fang et al., 2009; Vrionis et al., 2005).

The local aquifer consists of alluvial deposits from the nearby Colorado River and overlies the relatively impermeable Wasatch formation. The alluvium consists of predominantly loamy soil with unconsolidated gravel and cobbles, and extends approximately 6.5 m below the land surface (U.S. Department of Energy, 1999). Aquifer mineralogy is dominated by quartz and feldspar with lesser amount of clays and iron bearing minerals such as goethite, magnetite, and hematite (Campbell et al., 2012). An abundance of framboidal pyrite has also been reported in “naturally reduced zone” (NRZ) sediments that are composed of elevated concentrations of natural organic matter and reduced mineral phases, such as FeS_2. Exploratory drilling at the site suggests NRZ sediments comprise ca. 10% of the aquifer volume (Qafoku et al., 2014, 2009).

NRZ sediments are primarily associated with fine-grained, low hydraulic conductivity, diffusion-limited environments (Janot et al., 2016). In contrast, relatively high hydraulic conductivity (10 m day^{-1}), advection-dominated transport (average pore water velocity = 0.3 m day^{-1}) is observed in other parts of the floodplain aquifer (Williams et al., 2011; Yabusaki et al., 2011). Moreover, variations in geochemical, microbiological and mineral properties have been observed across the site depending upon local lithology (Campbell et al., 2012; Janot et al., 2016; Wainwright et al., 2015). Several studies have documented that the interaction of uranium, iron, sulfate and carbon species in NRZ sediments at the site is different than what is observed in visibly unreduced background aquifer sediments (Campbell et al., 2012; Flores Orozco et al., 2011; Qafoku et al., 2014). Therefore, this study investigated temporal patterns in conservative and redox-sensitive elements along distinct transects of the Rifle site (including both naturally reduced and unreduced zones).

At the site, the groundwater is shallow (about 3.5 m below ground surface) and flows in a south-southwest direction towards the river. Previous

investigations have reported the temporal variability of groundwater flow and direction within the Rifle site and also linked dissolved oxygen uptake rates to the seasonality of groundwater flow (Long, 2009; U.S. Department of Energy, 2012). The seasonality of the water table can be attributed to snowmelt runoff, recharge events, irrigation runoff, precipitation, and Colorado River stage variations (Fang et al., 2009; U.S. Department of Energy, 2012; 1999; Williams et al., 2011).

2.1.1. Site characteristics

Multiple factors potentially contribute to the temporal variability observed in biogeochemical parameters at the Rifle Site, including weather conditions, vegetation factors, and both natural and engineered hydrologic features that preferentially distribute water at the site. To account appropriately for the underlying mechanisms controlling this temporal variability, salient features of the Rifle site conditions were considered in this study.

The Rifle floodplain region has an arid to semiarid climate, and the character of rainfall is seasonally variable. During the summer, rainfall occurs in high-intensity, short-duration thunderstorms, and during the winter, precipitation occurs primarily in the form of snowfall. On an average, the region is characterized by cold winters, hot summers, large diurnal and seasonal temperature variations, low precipitation, and high evaporation rates (U.S. Department of Energy, 1999). Potential evaporation for the Rifle site occurs mainly from April through October, with a maximum in July (U.S. Department of Energy, 1999). Vegetation at the site is shallowrooted and dominated by tall and western wheatgrass. Hydrologic features near the site consist of the City of Rifle's detention lagoons to the northeast (above the site), several seeps and springs (off-site), surface irrigation runoff ditches to the north (above the site), and a partially unlined irrigation return ditch that bisects the site before discharging to the Colorado River (Fig. 1b) (U.S. Department of Energy, 1999). Among these features, the seeps discharge seasonally while springs provide water throughout the year. Irrigation discharges are also seasonal in operation from April through November of each year. The water stage for the Colorado River increases during the high-runoff months of April through June (U.S. Department of Energy, 2012). The groundwater flow system is also temporally dynamic, as suggested above.

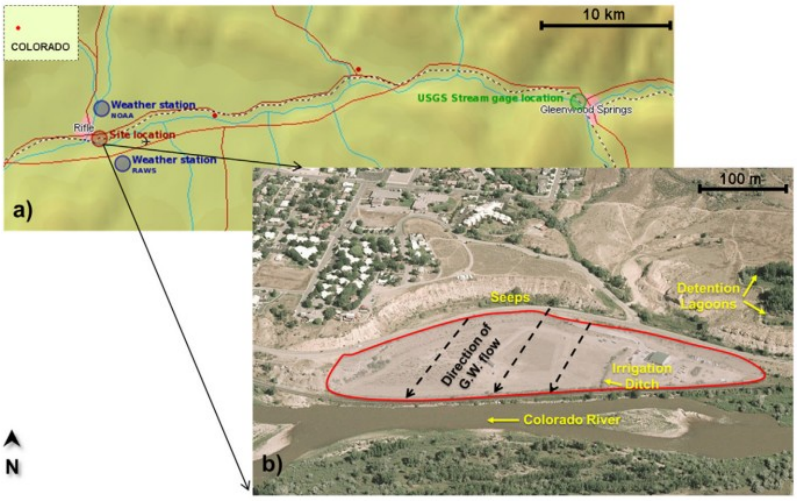

Fig. 1. a) Geographic location of the Rifle study site, the weather station, and USGS stream gaging stations, and b) hydrologic features at and in the vicinity of the site. G.W. refers to groundwater.

2.2. Data description

2.2.1. Geochemical dataset

Data from three transects of the Rifle site were chosen for analysis in this study (Fig. 2). The transects were chosen based on the availability of temporally resolved data and their locations in regions of the floodplain previously recognized to have distinct hydrological and biogeochemical characteristics. One transect of wellbores samples groundwater from a part of the floodplain aquifer that has the highest uranium concentration, a second transect traverses a naturally reduced zone within the aquifer, and the third transect focuses on samples collected from seeps emanating from an outcrop that forms the upgradient boundary of the Rifle floodplain.

The contaminated transect consists of five wells (310, U-01, B-01, 655, and LQ-109) with the highest uranium and vanadium concentrations reported during the time frame of analysis (January 2011–May 2013). These fully penetrating and screened wells are located on a transect parallel to the groundwater flow (Fig. 2). The seep transect includes multiple seeps (KHW1, KHW3, KHW4, and KHW5) immediately north of the site that are sustained by groundwater passing through upgradient, higher elevation sediments; the seeps also contribute flow to the onsite irrigation return ditch (U.S. Department of Energy, 2012). The unlined irrigation return ditch bisects the site and contributes to aquifer recharge. Given the inferred importance of seeps to aquifer recharge at the site, temporally resolved geochemical samples obtained along the seep transect are used for this study. The naturally reduced zone includes three wells (309, 310, and 304) located in a region exhibiting aqueous geochemical parameters reflective of reducing conditions, such as elevated Fe(II) and persistently low dissolved oxygen. The NRZ represents an opportunity to study localized zones of contrasting mineralogy, microbial activity, and redox conditions as compared to unreduced background sediments that predominate over most of the site.

Wavelet analysis was performed on data collected between 2011 and 2013 along the contaminated, seep, and naturally reduced transects (Table 1). This dataset contains geochemical constituents including Al, Cl, Fe, K, Na, Mg, Mn, Si, SO_4, $\delta^{34}S\text{-}SO_4$, V, and U at all sampling locations. Monthly data collected at multiple sampling locations along each transect resulted in approximately 100 data points for each constituent. A more detailed description of the sampling and analytical methods can be obtained from Williams et al. (2011). Briefly, samples for anion analysis were filtered (0.45 µM, PVDE) and stored in refrigerated, no-headspace HDPE vials for later analysis on an ion chromatograph (ICS-2100 equipped with an AS-18 analytical column, Dionex, CA). Samples for cation analysis were filtered and acidified with trace metal grade HNO3 for later analysis on ion coupled plasma mass spectrometry (ICP-MS) (Elan DRCII ICP-MS, Perkin Elmer, CA). Dissolved uranium was quantified using kinetic phosphorescence analysis (Chemchek Instruments, Richland, WA) or by ICP-MS analysis. Samples for $\delta^{34}S\text{-}SO_4$ were immediately filtered through 0.2 µM PTFE filters into vials containing $BaCl_2$ in excess of background sulfate concentrations (to precipitate $BaSO_4$) for later isotopic analysis on an elemental analyzer (Model 3028, Eurovector, CA) as described by Druhan et al. (2012). Sulfur isotopic analysis was carried out following the method of Giesemann et al. (1994) and isotopic ratios were reported in standard delta notation relative to the Canyon Diablo Troilite standard.

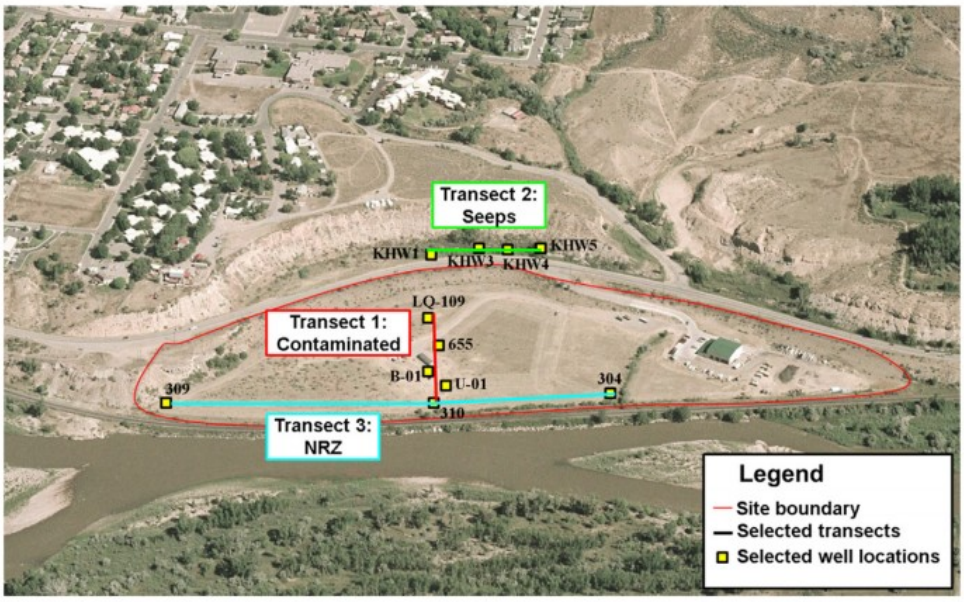

Fig. 2. The three transects and the corresponding sampling locations used for analysis at the Rifle site. NRZ refers to the naturally reduced zone.

2.2.2. Meteorological and hydrological datasets

There are several distinct features of the site that represent potentially important drivers of temporal variability for biogeochemical processes at the site. Therefore, data on weather variables (precipitation, temperature, and

humidity), vegetation indicators (potential evapotranspiration), water table depth variations, irrigation water withdrawal and river stage fluctuations were used in Shannon entropy analysis to identify the controls governing geochemical hot moments at the site.

Historical information about meteorological variables including total precipitation, relative humidity, and air temperature, was obtained from the Western Regional Climate Center (http://www.raws.dri.edu/cgi-bin/rawMAIN.pl?coCRIF) for the Remote Automatic Weather Station (RAWS) at Rifle, CO (Latitude 39.512°N, Longitude 107.749°W), which is located nearest to the study site at 6120 ft elevation (Fig. 1a). This weather station also provides estimates of Penman evapotranspiration values, which can act as a useful indicator for vegetation dynamics at the site. To account for temporal changes in precipitation, separate information on rainfall and snowfall data was obtained from NOAA from the Global Historical Climatology Network-Daily station (ID: US1COGF0002) located 0.9 NE of Rifle, CO (Fig. 1a). Note that multiple stations were selected as they were representative of site conditions and provided different meteorological variables.

Table 1
Sampling frequency for different transects of the Rifle site for wavelet analysis.

	Number of sampling locations	Total number of data points for each geochemical constituent	Analyzed sampling dates
Contaminated zone	5	145	January 2011 – May 2013
Seep zone	4	136	January 2011 – October 2013
Naturally reduced zone (NRZ)	3	87	January 2011 – May 2013

Many different datasets were used to document the natural and hydrological aspects of the study site, including data associated with the Colorado River, groundwater table, and irrigation sources from upstream and upslope areas. Discharge data on the Colorado River was obtained from the nearest U.S. Geological Survey (USGS) gaging station (ID: 09085100) (Fig. 1a). Water level observations from the screened monitoring wells at the Rifle site were also used in this study. Since irrigation withdrawal and consumption data from upstream sources was lacking, relative information on seasonal irrigation demand and how this demand changed from 2011 to 2013 were used (see Appendix A for more information).

3. Methods

Wavelet and Shannon entropy approaches were applied to the datasets described in Section 2. A brief description of these approaches is provided here and further details are included in Appendix B.

3.1. Wavelet analysis

Wavelet analysis was used to identify geochemical hot moments in the Rifle datasets. To characterize the time-dependence of the Rifle geochemical datasets, the continuous wavelet transform (CWT) was used. CWT is a filtering approach that decomposes the data in both time and frequency domains using a wavelet function (Foufoula-Georgiou and Kumar, 1994;

Guan et al., 2011). Although a wide variety of wavelet functions exist in the literature, we used the Morlet wavelet (with $\omega_0 = 6$) because it has the ability to capture oscillatory behavior and has been shown to correctly identify modes of variability in geochemical time series (Arora et al., 2013; Grinsted et al., 2004; Henderson et al., 2009; Janicke et al., 2009).

Wavelet coefficients W_D from CWT were used to visualize the variance of the time series by developing the local and global wavelet power spectra. The boundaries of the local wavelet power spectrum are referred to as the cone of influence that are usually excluded from the wavelet analysis (Guan et al., 2011). While the local power spectrum is useful to determine the dominant scales of variation in both time and frequency domains, the global power spectrum identifies the dominant peaks or hot moments of the geochemical time series. We used a 10% significance level to determine the statistical significance of both the local and global wavelet spectra in this study.

To interpret how geochemical constituents co-vary in time, the cross-wavelet transform was employed. The wavelet crossspectrum is analogous to the covariance function such that the modulus of the wavelet cross-spectrum quantifies the power and phase angle represents the delay in the time-dependent relationship between the variables (Labat et al., 2000; Maraun and Kurths, 2004). For the Rifle dataset, wavelet cross analyses on two geochemical constituents can provide meaningful information on the common interaction or processes affecting these variables.

In addition, multilevel decomposition (MLD) was used to examine the Rifle datasets at a detail matched to their scale, thus providing the opportunity to identify geochemical hot moments ranging from localized to long-term scales (Arora et al., 2013; Lau and Weng, 1995; Quiroz et al., 2011). This is possible because MLD splits the original time series data into approximate (smooth) and detailed (noise) components at discrete time intervals (Arora et al., 2013; Quiroz et al., 2011). Daubechies 5 (Db5) wavelet and scaling functions were used to analyze the Rifle datasets. For this study, the approximate coefficients at time intervals where hot moments expressed themselves were combined with entropy statistics to determine the processes causing these hot moments.

3.2. Entropy analysis

Shannon entropy methods were used to associate these hot moments with transport and/or biogeochemical factors. Since entropy-based measures are usually based on single-scale analysis, we combined information metrics with wavelet analysis to relate the information and structure of these processes to the resulting temporal variability of the geochemical constituents. In particular, mutual information (MI) can be used to relate geochemical hot moments to meteorological variables, hydrologic interactions and vegetation structure without any assumptions on the nature of this dependence (Kumar and Ruddell, 2010; Maes et al., 1997). If mutual information is 0, it implies that no additional information is available in the joint probability of the two

variables as compared to the individual datasets (Butte and Kohane, 2000). As mutual information increases, it signifies the strength of the relationship between the two datasets. For the Rifle site, mutual information was used to quantify the statistical dependence between the time series of a geochemical variable (using approximate coefficients at discrete time scales) and individual components like weather, vegetation or hydrologic datasets.

4. Results and discussions

Wavelet and entropy techniques described in the previous sections were used to investigate the time series behavior of a suite of geochemical constituents in the contaminated, seep and naturally reduced zones of the Rifle floodplain. We applied the approaches to gain insights into the distribution and causes of geochemical hot moments along distinct transects within the Rifle floodplain. Although our approaches were applied to the entire dataset, we selected subsets of the constituents to illustrate results associated with the different transects. Additional results are shown in Appendix C.

4.1. Distribution and controls of hot moments in the contaminated zone

Fig. 3 depicts the time series data as well as local and global wavelet spectra of sulfate, chloride, vanadium, and manganese in the contaminated zone of the Rifle site using the Morlet wavelet. The cone of influence is marked with the crosshatched regions in the local wavelet spectrum and is excluded from this discussion. Based on the Morlet wavelet, all four time series depict two dominant scales of variations in their local wavelet spectra - at 2 and 4–6 month periods (black contours, Fig. 3b). The black contours enclose regions of greater than 90% confidence based on a white noise background spectrum (Appendix B, Eq. (5)). These dominant scales of variations are associated with high concentrations as is evident from the time series profiles (Fig. 3a). Interestingly, the 4–6 month frequency is also evident in the global wavelet spectra (Fig. 3c) for all four geochemical constituents while the 2 month frequency is visible only for the reactive species (vanadium and manganese) at the 10% significance level. This indicates that the 2 month frequency constitutes a geochemical hot moment for reactive species only. While these short-term frequencies for manganese and vanadium could be indicative of redox cycling due to hydrologic perturbations, a more robust quantification of this behavior is explored using entropy analysis.

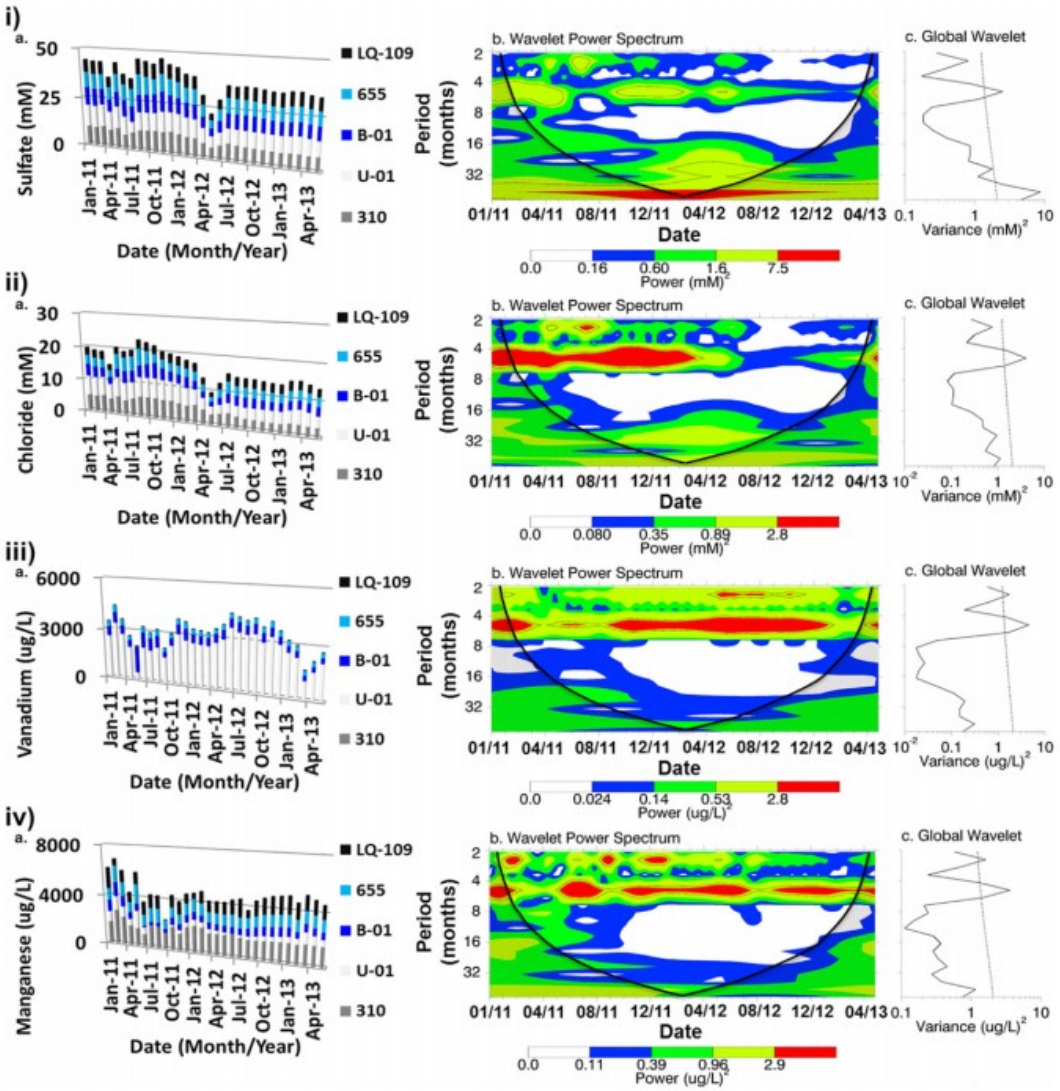

Fig. 3. (a) Time series, (b) local and (c) global wavelet spectrum of i) sulfate, ii) chloride, iii) vanadium, and iv) manganese in the contaminated zone of the Rifle floodplain. In the local wavelet spectrum, the cone of influence is delineated by a bold black line and excluded from the analysis, the contour levels are chosen such that 75%, 50%, 25%, and 5% of the wavelet power is above each level, respectively, and the black contour is the 10% significance level using a white-noise background spectrum. In the global wavelet spectrum, dashed line is the 10% significance level using a white-noise background spectrum.

It is interesting to note that the 4–6 month dominant frequency (black contours) is more transient for sulfate and chloride than for their reactive counterparts in the local wavelet spectra (Fig. 3b). A common time frame of this discontinuity is visible beyond June 2012 for both sulfate and chloride. Note that the time series profiles (Fig. 3a) also show a decrease in sulfate and chloride concentrations beyond June 2012. The explanations for this transient behavior will also be explored using entropy analysis.

Another thing to note is that sulfate time series behaves conservatively in the Rifle floodplain because of the presence of high sulfate concentrations in groundwater entering the floodplain and the extent of natural sulfate reduction not being significant enough to change these high concentrations. Fig. 3i and ii show that chloride and sulfate are correlated with each other

between 2011 and 2013. This is also evident in the wavelet cross spectrum of chloride and sulfate (Fig. 4). The wavelet cross spectrum is used in this study to describe the strength of this correlation in the timefrequency space. Fig. 4a represents the modulus of the wavelet cross spectrum and suggests that both signals have strong correlation (red contours) at 4 months and significant correlation (green contours) at 5 months and between 18 and 32 months. Fig. 4b further reveals that these contours are discontinuous in time, which indicates the quasi-periodic nature of this relationship. Fig. 4b represents the phase angle of the wavelet cross spectrum and again suggests that the relationship between sulfate and chloride signals is time-dependent. This time-dependent behavior indicates that sulfate and chloride concentrations are possibly impacted by similar hydrologic perturbations but have different sources or sinks.

Comparatively, time series data on $\delta^{34}S\text{-}SO_4$ is much more indicative of redox behavior at the Rifle site due to the sensitivity of this isotope to even modest levels of reaction (e.g. sulfate reduction by microorganisms) (Druhan et al., 2012). Fig. 5 shows the time series and wavelet spectra of $\delta^{34}S\text{-}SO_4$ between 2011 and 2013 using the Morlet wavelet. As with other redox sensitive species, two dominant scales of variation at 2 and 4–6 month periods are evident in both the local and global wavelet spectra of $\delta^{34}S\text{-}SO_4$. Fig. 5b further depicts that the 4–6 month frequency (black contour) is more continuous as with other redox sensitive species, and displays a discontinuity only between May–July 2012. Furthermore, Fig. 6 shows the wavelet cross spectrum of $\delta^{34}S\text{-}SO_4$ and sulfate. Fig. 6a indicates that both signals have strong correlation (red contours) at 4 months and significant correlation (green contours) at 5 months and between 25 and 32 months. In particular, the strength of this relationship at scale 2 is weak, which is represented by blue contours. The time series profiles (Figs. 3a and 5a) as well as the modulus and phase angle plots (Fig. 6) again reveal a time varying correlation between the two signals. More importantly, the 2 month frequency observed in reactive species like manganese, vanadium, and $\delta^{34}S\text{-}SO_4$ (a more sensitive proxy for sulfur cycling, such as sulfate reduction) is not visible in the bulk sulfate concentration time series. Thus, bulk sulfate will be treated as a conservative indicator of flow dynamics in this study.

Entropy analysis was performed to identify the transport and biogeochemical factors influencing geochemical hot moments at 2 and 4–6 month frequencies in the contaminated zone of the floodplain. As described above, multilevel decomposition is conducted on the geochemical time series that removes the noise (detailed components) from the data and keeps only the approximations at each scale. As only dyadic scales of 2 are possible, approximations at 2 and 4 month scales are compared with site data on weather dynamics, vegetation indicators, and hydrologic conditions to extract the mutual information between them (Table 2). Table 2 displays the MI between conservative (sulfate, chloride) and redox-sensitive species (manganese) and different site features at 4 month scales. Table 2 shows

that all three variables have high mutual information (MI) with snowfall (0.4–0.7). This relatively high MI signifies that temporal variability in different geochemical constituents at 4 months is related to snowfall events. The local wavelet spectra (Fig. 3b) also suggest that the 4 month frequency consistently expresses itself during snowfall months of January–April 2011 and November 2011–February 2012 for all four geochemical constituents. The reasons for an inconsistent behavior of this 4 month frequency during the snowfall months of 2012–13, especially for conservative species, are discussed below. Table 2 further shows Penman evapotranspiration and total precipitation to have significant MI (0.3–0.4) with both conservative and reactive species at 4 months.

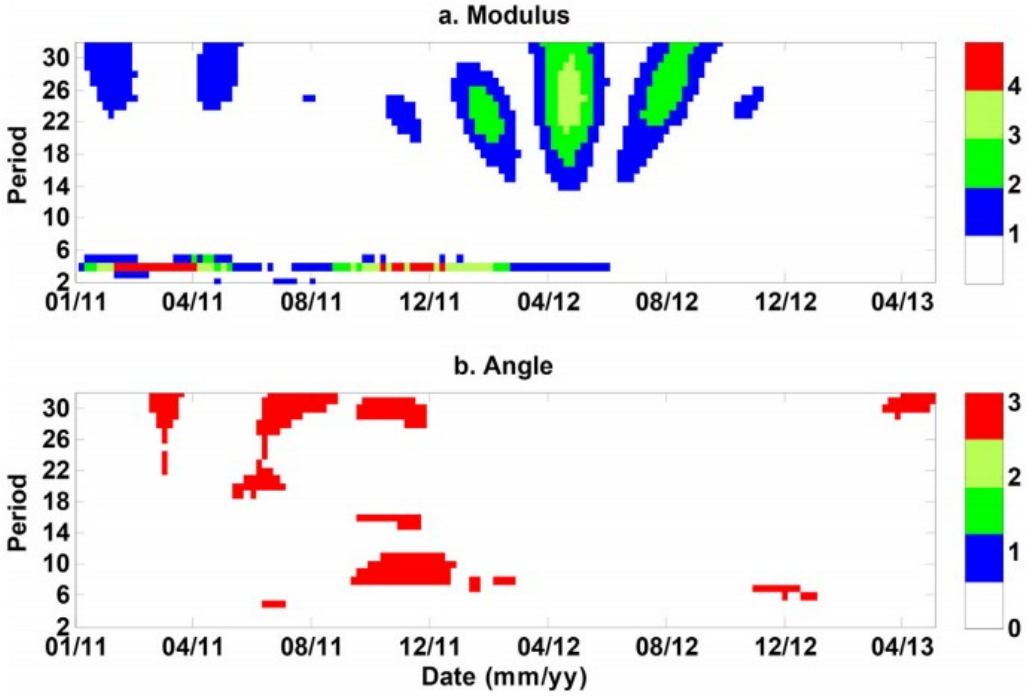

Fig. 4. (a) Modulus and (b) angle of the wavelet cross spectrum of sulfate and chloride in the contaminated zone of the Rifle floodplain.

The mutual information is thus able to establish a flow of information between chloride and sulfate and precipitation and hydrologic features of the site revealing two interesting points. First, the discontinuity observed in the local power spectrum of chloride and sulfate beyond June 2012 (Fig. 3i and ii) could be a result of the fact that hydrological conditions in 2012 were significantly different from 2011, with the region facing a severe drought in 2012 (Hoerling et al., 2014). Second, periodicity in sulfate and chloride data varies between 4 and 6 months potentially as the result of precipitation changes in this region. As suggested earlier, winters are dry with precipitation occurring as snow, spring season is marked with gentle rainfall or wet snow, summer season has lowhumidity with the threat of high-intensity, short-duration rainfall thunderstorms, and fall season is usually

dry. A deeper analysis of frequency correlation with precipitation is provided in section 4.4.

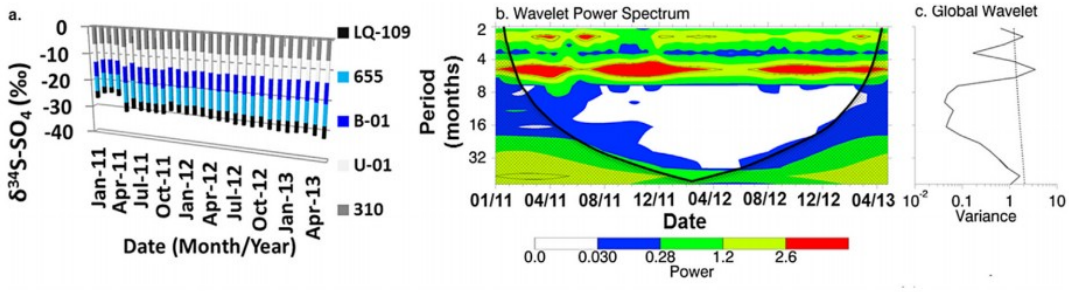

Fig. 5. (a) Time series, (b) local and (c) global wavelet spectrum of $\delta^{34}S\text{-}SO_4$ in the contaminated zone of the Rifle floodplain. In the local wavelet spectrum, the cone of influence is delineated by a bold black line and excluded from the analysis, the contour levels are chosen such that 75%, 50%, 25%, and 5% of the wavelet power is above each level, respectively, and the black contour is the 10% significance level using a white-noise background spectrum. In the global wavelet spectrum, dashed line is the 10% significance level using a white-noise background spectrum.

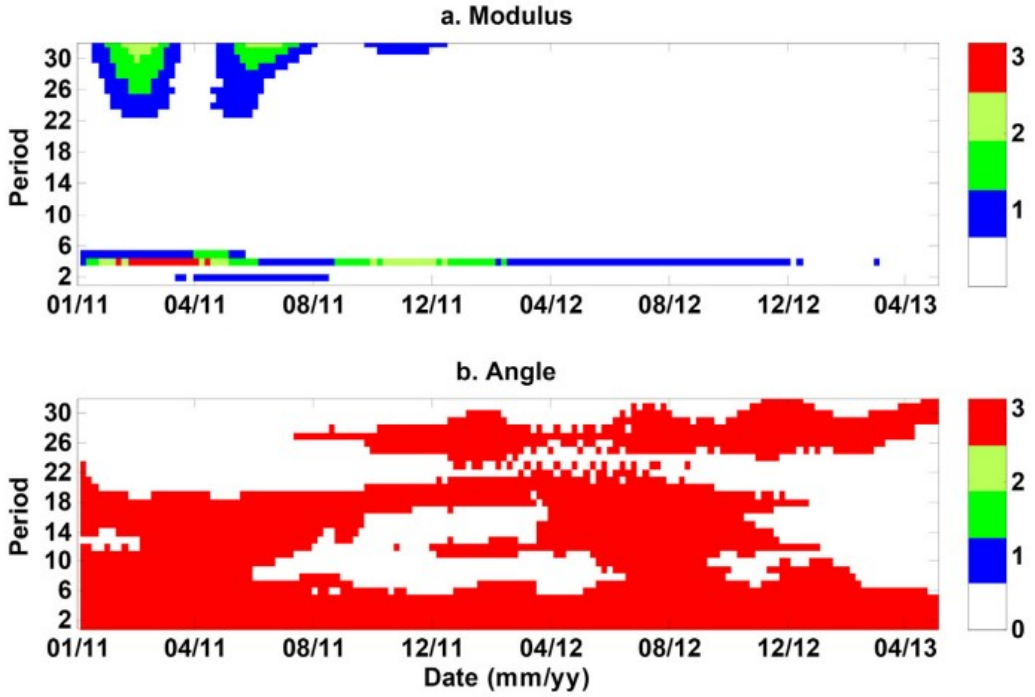

Fig. 6. (a) Modulus and (b) angle of the wavelet cross spectrum of sulfate and $\delta^{34}S\text{-}SO_4$ in the contaminated zone of the Rifle floodplain.

Table 2
Mutual information for wavelet coefficients at 4 month scale for different geochemical constituents and site components in the contaminated zone of the Rifle site.

Dataset source	Dataset type	Chloride	Sulfate	Manganese
RAWS	Total precipitation	0.36	0.34	0.35
	Average temperature	0.24	0.22	0.24
	Humidity	0.22	0.24	0.23
	Penman evapotranspiration	0.38	0.29	0.44
NOAA	Rainfall	0.18	0.17	0.21
	Snowfall	0.40	0.60	0.66
USGS	Daily discharge	0.33	0.33	0.25
Site observation	Depth to groundwater	0.12	0.26	0.20
Qualitative	Irrigation withdrawal	0.22	0.28	0.20

Table 3
Mutual information for wavelet coefficients at 2 month scale for different geochemical constituents and site components in the contaminated zone of the Rifle site.

Dataset source	Dataset type	Manganese	Vanadium
RAWS	Total precipitation	0.38	0.40
	Average temperature	0.19	0.18
	Humidity	0.19	0.18
	Penman evapotranspiration	0.16	0.10
NOAA	Rainfall	0.13	0.13
	Snowfall	0.21	0.19
USGS	Daily discharge	0.20	0.50
Site observation	Depth to groundwater	0.03	0.05
Qualitative	Irrigation withdrawal	0.13	0.20

Table 3 displays the MI between redox-sensitive species (manganese, vanadium) and different site components at 2 month scales. Table 3 indicates that periodicity in redox-sensitive species at 2 months is related to rainfall events with a significant MI (≈0.4). Interestingly, vanadium also shows a strong dependency (MI = 0.5) to USGS discharge data at 2 month scales, but this flow of information is weak for manganese (MI = 0.2). The large codependency between vanadium and USGS hydrological profiles could be due to the presence of large vanadium deposits in the area and existing background concentrations (Fischer and Botinelly, 1960). This codependency is thus indicative of transport-driven hot moments.

In summary, both conservative and redox-sensitive species in the contaminated zone of the floodplain revealed a 4–6 month periodicity, while reactive species showed an additional 2 month periodicity between 2011 and

2013. Both of these frequencies were found to be transport-driven and correlated with hydrologic variations in snowfall and precipitation data.

4.2. Distribution and controls of hot moments in the seep zone

Fig. 7 illustrates the time series, local and global wavelet spectra of chloride, sulfate, $\delta^{34}S\text{-}SO_4$, and potassium in the seep zone of the Rifle floodplain. Note that a longer dataset spanning January 2011–October 2013 was used for this zone (Table 1). A 32 month frequency is visible in the local wavelet spectra for all four time series data as represented by the black contours with 90% confidence level (Fig. 7b). In addition, several other frequencies that show time localization are visible in the local power spectra, such as a 4 month frequency in the local power spectrum of sulfate (Fig. 7ii) occurs between December 2012 and January 2013. Similarly, the local wavelet spectrum of chloride reveals high power wavelet coefficients (indicated by black contours) across scales 2–32 between August and September 2012, while potassium reveals these multiscalar (scales 4–16), high power wavelet coefficients in May 2011 and August 2013. Note that these high wavelet coefficients are associated with high concentrations as is evident from the time series profiles (Fig. 7a). However, only the 32 month frequency shows dominance at the 10% significance level in the global wavelet spectra (Fig. 7c) for all four geochemical constituents. Another frequency prominent in the global wavelet spectra of reactive species (manganese, $\delta^{34}S\text{-}SO_4$) occurs at 12–16 month scales. In the local wavelet spectra, this 12–16 month frequency is evident between January 2011 and February 2013 for $\delta^{34}S\text{-}SO_4$, but is localized to the first year of study (until August 2011) and reappears in March 2013 for potassium. Although potassium concentration profiles could be indicative of weathering processes, ion exchange reactions, or microbial biomass, other redox-sensitive species such as vanadium and manganese also show time localized frequency at 12–16 months in their local wavelet spectra (not shown here) similar to potassium. The reasons for this mismatch in behavior are analyzed using entropy analysis.

Entropy analysis was again used to evaluate the causes for hot moments at 12–16 and 32 month scales of different geochemical constituents in the seep zone of the Rifle floodplain. After removing the noise components, the approximate coefficients of both conservative and reactive geochemical constituents at 32 months were again compared with several site components using mutual information criterion. Table 4 reveals that a very high flow of information (MI = 0.5–0.8) exists between depth to groundwater and different geochemical constituents in the seep zone. Penman evapotranspiration also has a high MI (0.4–0.6) with the geochemical constituents at this scale. Interestingly, sulfate reveals significant co-dependency (MI ≈ 0.5) with several site components like precipitation, temperature, humidity, and USGS discharge, as well as irrigation withdrawal.

Table 5 shows the mutual information between approximations of reactive species (vanadium, manganese, potassium, and $\delta^{34}S\text{-}SO_4$) at 16 months and

site components. For vanadium, manganese and potassium, a very high MI (0.7–0.8) is again observed with groundwater dynamics at this scale and significant MI (0.5–0.6) is obtained with precipitation and evapotranspiration components. Comparatively, mutual information of $\delta^{34}S\text{-}SO_4$ shows high MI (≈0.5) with precipitation and evapotranspiration components, but not with depth to groundwater. Instead, a larger flow of information (MI = 0.5–0.6) is obtained between rainfall and snowfall events and $\delta^{34}S\text{-}SO_4$ time series at 16 months. In this sense, the inconsistency obtained with 12–16 month frequencies observed in the local wavelet spectra of potassium (Fig. 7iv) and $\delta^{34}S\text{-}SO_4$ (Fig. 7iii) can be understood. Entropy analysis suggests that different controls affect $\delta^{34}S\text{-}SO_4$ and other reactive species at 16 months. This could be indicative of different sources of sulfate and other reactive species (such as, aquifer solids, background groundwater), or different biogeochemical factors controlling their concentrations (such as microbial uptake affecting potassium concentrations, iron mineral interactions with sulfate/sulfide).

In summary, conservative and redox sensitive species in the seep zone of the Rifle floodplain revealed a 32 month periodicity that was correlated with several hydrologic features like depth to groundwater, Penman evapotranspiration and irrigation withdrawal. We believe that geochemical hot moments in the seep zone are transport-driven and impacted by the net residence time of groundwater. In addition, reactive species like manganese and $\delta^{34}S\text{-}SO_4$ revealed another dominant frequency at 12–16 month scales. This frequency was strongly correlated with annual hydrologic variations at the site (transport-related hot moments), but revealed significant differences in processes controlling redox cycling for different species (biogeochemically-driven hot moments).

4.3. Distribution and controls of hot moments in the naturally reduced zone

Fig. 8 demonstrates the time series, local and global wavelet spectra of chloride, sulfate, vanadium, and uranium in the naturally reduced zone of the Rifle floodplain. The local wavelet spectra (Fig. 8i-iv) show a single dominant scale of variation at 3 months for both conservative and reactive species. This 3 month frequency (represented by black contours) is statistically significant in the local wavelet spectra (Fig. 8b) and also shows dominance in the global wavelet spectra (indicated by dashed lines in Fig. 8c) at 90% confidence levels based on the white noise background spectrum. To further confirm that a single dominant frequency is evident in the wavelet spectra of different geochemical constituents in the NRZ, we analyzed temporal characteristics of uranium and vanadium for a longer dataset spanning 16 years of observations (1998–2014). Fig. 9 shows that this 3 month frequency is still statistically significant in both the local and global spectra of uranium and vanadium. Note that this dominant frequency is continuous throughout the short time period of analysis for uranium only (Fig. 8iv) and shows discontinuity at different times for uranium in the 16 year dataset (Fig. 9i and ii) as well as for all other variables in the local power spectra (Fig. 8i-iii). In

particular, chloride displays this discontinuity before April 2011 and beyond December 2011, sulfate between April and June 2011, and vanadium between March and June 2011 in Fig. 8b.

To further evaluate the factors affecting hot moments at 3 month scales in the naturally reduced zone of the Rifle floodplain, mutual information criterion is used. A multilevel decomposition is conducted on both conservative and reactive species to obtain approximate coefficients at both 2 and 4 months, which are then compared with several site features (Table 6). Table 6 shows that USGS discharge data has a high MI (≈0.6) with sulfate and significant MI (0.3–0.4) with vanadium and chloride. However, the flow of information between USGS hydrological profiles and other geochemical constituents is weak (MI = 0.1–0.2). Table 6 also reveals that there is no particular site component that demonstrates a consistent MI behavior with the different geochemical constituents although they all have a common dominant scale of variation in the NRZ. For example, Penman ET has significant MI (≈0.3) with chloride and manganese, but not with other geochemical constituents. This mismatch in the transport and biogeochemical factors dominating the hot moments in the NRZ could be the reason for disparity in time localization of the 3 month frequency in their local wavelet spectra. The lithological characteristics (high organic carbon, elevated concentrations of reduced iron and metal sulfide phases) in this zone of the floodplain are interpreted to be a predominant control on hot moment behavior relative to seasonal hydrologic variations or residence time of groundwater in contrast to the other two locations (non-NRZ contaminated and seep zones). This has been corroborated by previous site investigations that have demonstrated that site-specific characteristics of NRZs are a dominant control on uranium bioreduction rates, oxygen consumption and dissolved iron concentrations (Arora et al., 2016; Bao et al., 2014; Bargar et al., 2011; Long, 2009).

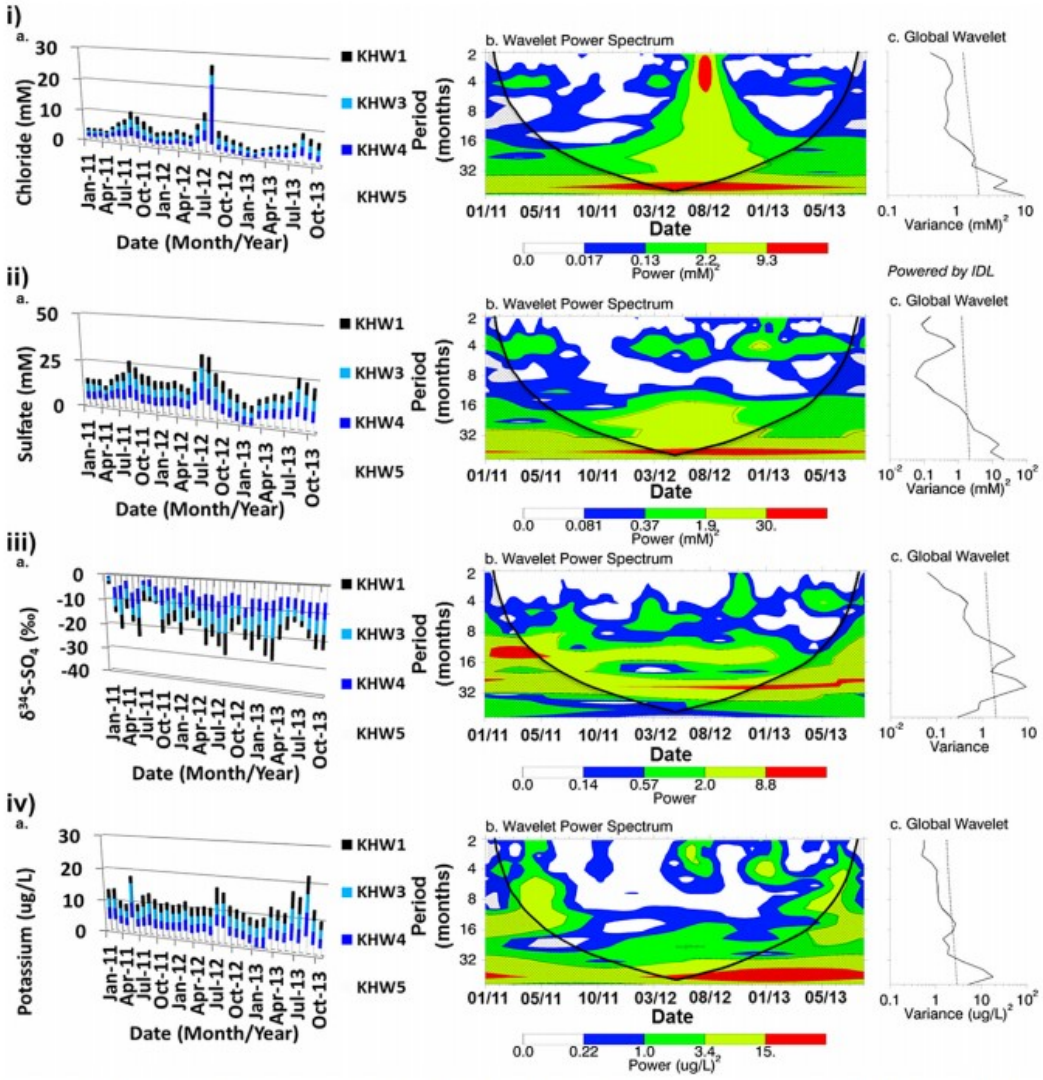

Fig. 7. (a) Time series, (b) local and (c) global wavelet spectrum of i) chloride, ii) sulfate, iii) δ^{34}S-SO_4, and iv) potassium in the seep zone of the Rifle floodplain. In the local wavelet spectrum, the cone of influence is delineated by a bold black line and excluded from the analysis, the contour levels are chosen such that 75%, 50%, 25%, and 5% of the wavelet power is above each level, respectively, and the black contour is the 10% significance level using a white-noise background spectrum. In the global wavelet spectrum, dashed line is the 10% significance level using a white-noise background spectrum.

Table 4
Mutual information for wavelet coefficients at 32 month scale for different geochemical constituents and site components in the seep zone of the Rifle site.

Dataset source	Dataset type	Chloride	Sulfate	Vanadium
RAWS	Total precipitation	0.31	0.61	0.28
	Average temperature	0.53	0.56	0.38
	Humidity	0.40	0.53	0.40
	Penman evapotranspiration	0.56	0.59	0.40
NOAA	Rainfall	0.34	0.31	0.28
	Snowfall	0.30	0.24	0.24
USGS	Daily discharge	0.49	0.51	0.40
Site observation	Depth to groundwater	0.70	0.88	0.55
Qualitative	Irrigation withdrawal	0.41	0.55	0.34

Table 5
Mutual information for wavelet coefficients at 16 month scale for different geochemical constituents and site components in the seep zone of the Rifle site.

Dataset source	Dataset type	Manganese	Vanadium	Potassium	$\delta^{34}S\text{-}SO_4$
RAWS	Total precipitation	0.65	0.76	0.42	0.50
	Average temperature	0.33	0.31	0.35	0.35
	Humidity	0.38	0.34	0.36	0.40
	Penman evapotranspiration	0.62	0.56	0.53	0.47
NOAA	Rainfall	0.25	0.28	0.46	0.60
	Snowfall	0.20	0.25	0.29	0.52
USGS	Daily discharge	0.45	0.42	0.41	0.34
Site observation	Depth to groundwater	0.73	0.84	0.80	0.30
Qualitative	Irrigation withdrawal	0.31	0.26	0.41	0.40

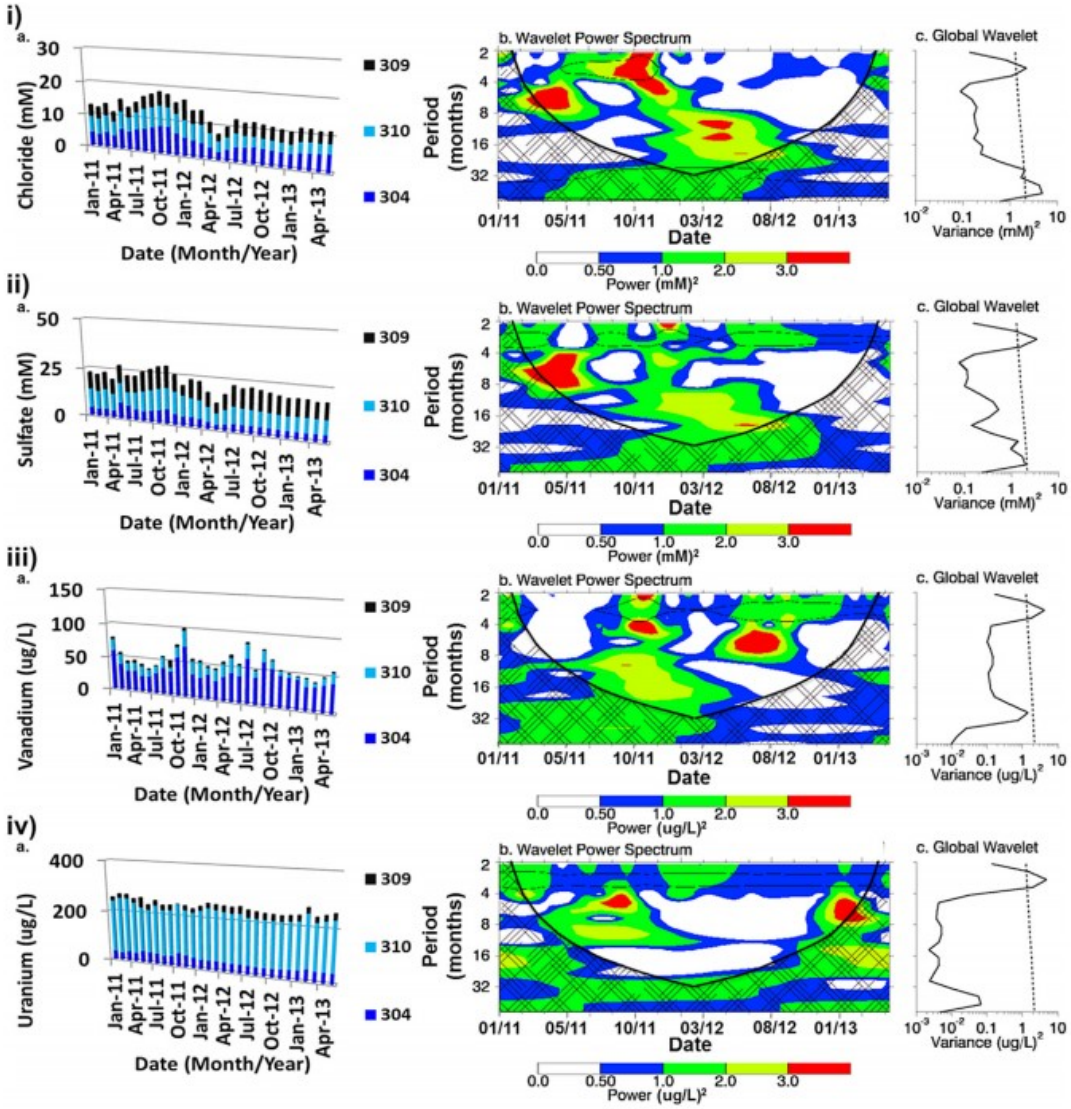

Fig. 8. (a) Time series, (b) local and (c) global wavelet spectrum of i) chloride, ii) sulfate, iii) vanadium, and iv) uranium in the naturally reduced zone of the Rifle floodplain. In the local wavelet spectrum, the cone of influence is delineated by a bold black line and excluded from the analysis, the contour levels are chosen such that 75%, 50%, 25%, and 5% of the wavelet power is above each level, respectively, and the black contour is the 10% significance level using a white-noise background spectrum. In the global wavelet spectrum, dashed line is the 10% significance level using a white-noise background spectrum.

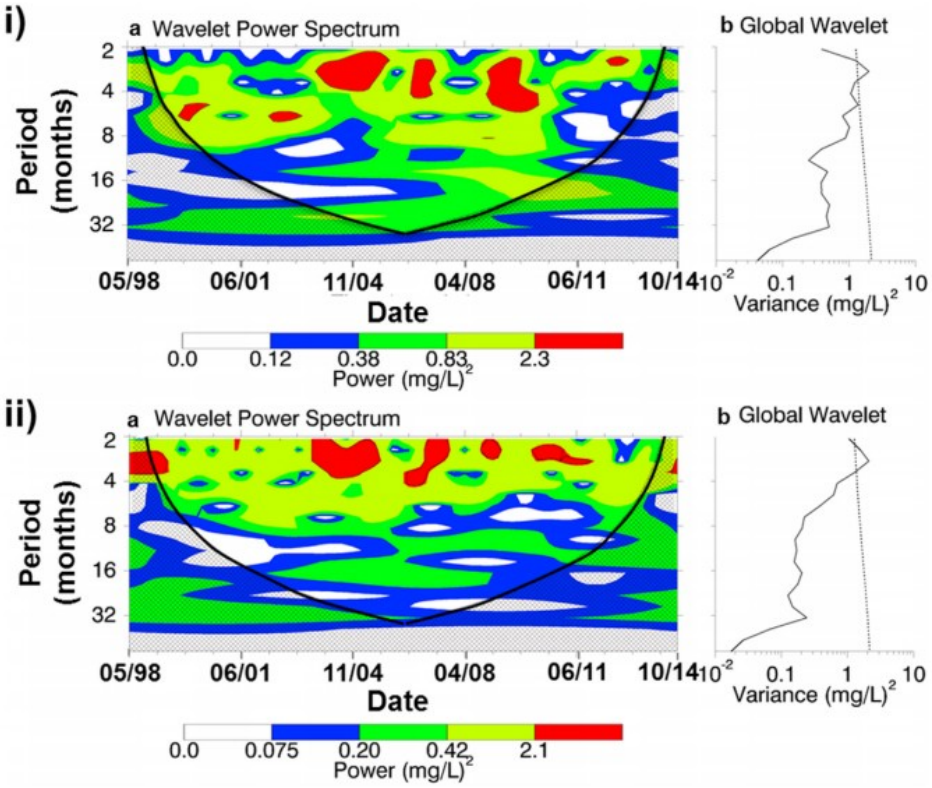

Fig. 9. (a) Local and (b) global wavelet spectrum of the longer time series of i) vanadium and ii) uranium in the naturally reduced zone of the Rifle floodplain. In the local wavelet spectrum, the cone of influence is delineated by a bold black line and excluded from the analysis, the contour levels are chosen such that 75%, 50%, 25%, and 5% of the wavelet power is above each level, respectively, and the black contour is the 10% significance level using a white-noise background spectrum. In the global wavelet spectrum, dashed line is the 10% significance level using a white-noise background spectrum.

Table 6
Mutual information for wavelet coefficients for different geochemical constituents and site components in the naturally reduced zone of the Rifle site.

Dataset source	Dataset type	Wavelet coefficients at 2 months			Wavelet coefficients at 4 months	
		Chloride	Sulfate	Uranium	Manganese	Vanadium
RAWS	Total precipitation	0.12	0.15	0.12	0.18	0.23
	Average temperature	0.23	0.24	0.24	0.24	0.23
	Humidity	0.21	0.18	0.15	0.20	0.21
	Penman evapotranspiration	0.34	0.27	0.18	0.32	0.20
NOAA	Rainfall	0.14	0.19	0.12	0.17	0.29
	Snowfall	0.12	0.20	0.19	0.16	0.33
USGS	Daily discharge	0.36	0.58	0.13	0.22	0.43
Site observation	Depth to groundwater	0.22	0.22	0.11	0.18	0.23
Qualitative	Irrigation withdrawal	0.24	0.23	0.09	0.18	0.19

This analysis showed that a single dominant frequency of 3 months is observed in the NRZ transect of the Rifle floodplain irrespective of conservative or reactive behavior of the geochemical constituents. Interestingly, this frequency was not correlated with seasonal hydrologic variations or groundwater dynamics, but suggested lithologic characteristics as the dominant control. This is similar to conclusions made in Hansen et al. (2011), which showed that lithological variability in the form of sand-over-loam layering significantly increased the rates of iron and sulfur cycling - due to iron oxide mineral crust formation and microbial colonization at the layered interface - as compared to homogeneous soil columns. Similarly, Salehikhoo and Li (2015) demonstrated that spatial heterogeneity in the

form of magnesite distribution patterns significantly impacted mineral dissolution rates in flow-through column experiments. Several studies have thus documented that lithological variations and subsurface heterogeneous properties can modify reaction rates and affect the distribution of geochemical concentrations.

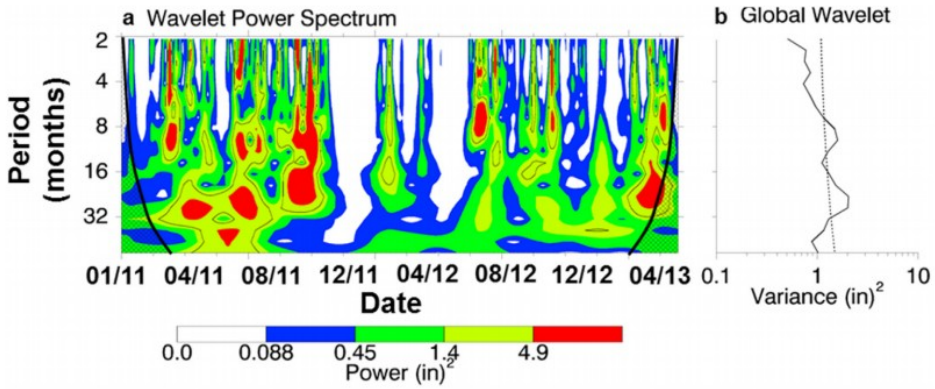

Fig. 10. (a) Local and (b) global wavelet spectrum of daily total precipitation from RAWS near the Rifle site. In the local wavelet spectrum, the cone of influence is delineated by a bold black line and excluded from the analysis, the contour levels are chosen such that 75%, 50%, 25%, and 5% of the wavelet power is above each level, respectively, and the black contour is the 10% significance level using a white-noise background spectrum. In the global wavelet spectrum, dashed line is the 10% significance level using a white-noise background spectrum.

4.4. Temporal characteristics of precipitation at the site

Since hydrologic variability presented an important control on hot moments in contaminated and seep zones of the site, we evaluated the continuous and global wavelet power spectrum of precipitation at the Rifle site using the Morlet wavelet (Fig. 10). The local wavelet spectrum shows that precipitation has multiscalar characteristics at 10% significance level (represented by black contours) during several time frames between 2011 and 2013. The global wavelet spectrum further reveals that precipitation has an annual (~12 months) and bi-annual (~24 months) periodicity at the 90% confidence level (represented by dashed lines in Fig. 10b). However, precipitation shows high mutual information with the geochemical constituents at scales different than annual, bi-annual, or other dominant frequency months (such as Tables 3 and 5). This shows that the aqueous geochemical data represent the aggregation of many geomorphic, hydrological, and biogeochemical processes, which interact at different scales. This further indicates that combining entropy with wavelet decomposition analysis presents a novel technique capable of discriminating the complex scale interactions between biogeochemical and hydrological processes that govern contaminant fate and transport in floodplains. This is also visible in the interactions between manganese and potential evapotranspiration, which show significant codependency (MI = 0.3–0.4) at 4 months (Tables 2 and 6), and relatively high flow of information (MI = 0.6) at higher time scales (Table 5) in the Rifle dataset. Therefore, this combined entropy-wavelet technique can be used to identify the dominant scales of interaction and underlying causes of hot moment behavior in geochemical datasets, and one that is readily applicable to other floodplain systems and hydrogeochemical datasets.

5. Conclusions

Contaminant fate and transport in riverine floodplains is characterized by temporal heterogeneity in hydrological, geochemical and microbial attributes, with consequences for nutrient cycling and water quality of their associated river systems. However, a systematic approach to decipher this temporal variability in complex multivariate datasets has been lacking. This study uses wavelets to identify temporal patterns or hot moments of geochemical activity along three transects of the Rifle floodplain, and combines wavelet decomposition analysis with entropy statistics to isolate the governing transport and/or biogeochemical processes driving these hot moments.

Wavelet and entropy analyses reveal that geochemical hot moments in both contaminated and seep zones are transportdriven. In particular, seasonal (4 month periodicity) hydrologic interactions constitute geochemical hot moments in the contaminated zone of the Rifle floodplain, and groundwater residence time (32 month periodicity) is the governing control on temporal variability in the seep zone. We found that reactive species portray additional hot moments than conservative species in both contaminated and seep zones. Comparatively, hot moments in the naturally reduced zone occur at 3 month scales for both conservative and reactive species demonstrating that the causes and distribution of hot moment behavior can be biogeochemically-driven and affected by heterogeneous lithological properties across the floodplain. A limitation of this analysis is that the linkages with hydrologic data are based on mutual information but lithological and biogeochemical associations are based on reasoning and knowledge from previous site investigations.

This study highlights how combining wavelet and entropy techniques can be used with temporal biogeochemical datasets to identify the distribution and governing processes of hot moments of contaminant activity. These combined metrics can be factored into predictive modeling of contaminant fluxes (e.g., Arora et al., 2016) and employed as decision making tools for water quality management. Although we applied the developed methods to a specific floodplain system, the wavelet-entropy approach should be readily transferrable to other terrestrial and aquatic ecosystems where a mechanistic understanding of the temporal interactions among biogeochemical and hydrological processes is desired.

Acknowledgments

This project was supported as part of the Subsurface Science Scientific Focus Area (SFA) funded by the U.S. Department of Energy, Office of Biological and Environmental Research to the Sustainable Systems SFA under award number DE-AC020SCH11231 and by the ASCEM project, which is supported by U.S. Department of Energy Environmental Management, under award number DEAC0205CH11231 to the LBNL.

Appendix A. Supplementary data

Supplementary data related to this article can be found at http://dx.doi.org/10.1016/j.envsoft.2016.08.005.

References

Anderson, R.T., Vrionis, H.A., Ortiz-Bernad, I., Resch, C.T., Long, P.E., Dayvault, R., Karp, K., Marutzky, S., Metzler, D.R., Peacock, A., White, D.C., Lowe, M., Lovley, D.R., 2003. Stimulating the in situ activity of Geobacter species to remove uranium from the groundwater of a uranium-contaminated aquifer. Appl. Environ. Microbiol. 69, 5884–5891.

Andrews, D.M., Lin, H., Zhu, Q., Jin, L., Brantley, S.L., 2011. Hot spots and hot moments of dissolved organic carbon export and soil organic carbon storage in the Shale Hills Catchment. Vadose Zo. J. 10, 943. http://dx.doi.org/10.2136/ vzj2010.0149.

Arora, B., Mohanty, B.P., McGuire, J.T., Cozzarelli, I.M., 2013. Temporal dynamics of biogeochemical processes at the Norman Landfill site. Water Resour. Res. 49, 6909–6926. http://dx.doi.org/10.1002/wrcr.20484.

Arora, B., S¸ engor, S.S., Steefel, C.I., 2015. A reactive transport benchmark on heavy € metal cycling in lake sediments. Comput. Geosci. 19, 613–633. http://dx.doi.org/ 10.1007/s10596-014-9445-8.

Arora, B., Spycher, N.F., Steefel, C.I., Molins, S., Bill, M., Conrad, M.E., Dong, W., Faybishenko, B., Tokunaga, T.K., Wan, J., Williams, K.H., Yabusaki, S.B., 2016. Influence of hydrological, biogeochemical and temperature transients on subsurface carbon fluxes in a flood plain environment. Biogeochemistry 127, 367–396. http://dx.doi.org/10.1007/s10533-016-0186-8.

Bao, C., Wu, H., Li, L., Long, P.E., Newcomer, D., Williams, K.H., 2014. Uranium bioreduction rates across scales: biogeochemical “hot moments” and “hot spots” during a biostimulation experiment at Rifle, Colorado. Environ. Sci. Technol. http://dx.doi.org/10.1021/es501060d.

Bargar, J.R., Campbell, K.M., Stubbs, J.E., Suvorova, E., Williams, K., LezamaPacheco, J.S., Blue, L.Y., Cerrato, J., Bernier-Latmani, R., Giammar, D.E., Long, P.E., 2011. Speciation and dynamics of biologically reduced uranium(IV) in the Old Rifle aquifer. Abstr. Pap. Am. Chem. Soc. 242.

Bradshaw, G.A., Spies, T.A., 1992. Characterizing canopy gap structure in forests using wavelet analysis. J. Ecol. 80, 205–215. http://dx.doi.org/10.2307/2261007.

Brunsell, N.A., Ham, J.M., Owensby, C.E., 2008. Assessing the multi-resolution information content of remotely sensed variables and elevation for evapotranspiration in a tall-grass prairie environment. Remote Sens. Environ. 112, 2977–2987. http://dx.doi.org/10.1016/j.rse.2008.02.002.

Butte, A.J., Kohane, I.S., 2000. Mutual information relevance networks: functional genomic clustering using pairwise entropy measurements. Pac. Symp. Biocomput 418–429. http://dx.doi.org/10.1142/9789814447331_0040.

Campbell, K.M., Kukkadapu, R.K., Qafoku, N.P., Peacock, A.D., Lesher, E., Williams, K.H., Bargar, J.R., Wilkins, M.J., Figueroa, L., Ranville, J., Davis, J.A., Long, P.E., 2012. Geochemical, mineralogical and microbiological characteristics of sediment from a naturally reduced zone in a uranium-contaminated aquifer. Appl. Geochem. 27, 1499–1511. http://dx.doi.org/10.1016/ j.apgeochem.2012.04.013.

Costa, M., Goldberger, A., Peng, C.-K., 2002. Multiscale entropy analysis of complex physiologic time series. Phys. Rev. Lett. 89, 068102. http://dx.doi.org/10.1103/ PhysRevLett.89.068102.

Druhan, J.L., Steefel, C.I., Molins, S., Williams, K.H., Conrad, M.E., Depaolo, D.J., 2012. Timing the onset of sulfate reduction over multiple subsurface acetate amendments by measurement and modeling of sulfur isotope fractionation. Environ. Sci. Technol. 46, 8895–8902. http://dx.doi.org/10.1021/es302016p.

Dwivedi, D., Mohanty, B., 2016. Hot spots and persistence of nitrate in aquifers across scales. Entropy 18, 25. http://dx.doi.org/10.3390/e18010025.

Fang, Y., Yabusaki, S.B., Morrison, S.J., Amonette, J.P., Long, P.E., 2009. Multicomponent reactive transport modeling of uranium bioremediation field experiments. Geochim. Cosmochim. Acta 73, 6029–6051. http://dx.doi.org/10.1016/ j.gca.2009.07.019.

Fendorf, S., Michael, H.A., van Geen, A., 2010. Spatial and temporal variations of groundwater arsenic in South and Southeast Asia. Science 328, 1123–1127. http://dx.doi.org/10.1126/science.1172974, 80-.

Fischer, R.P., Botinelly, T., 1960. Vanadium-uranium Deposits of the Rifle Creek Area, Garfield County, Colorado. Flores Orozco, A., Williams, K.H., Long, P.E., Hubbard, S.S., Kemna, A., 2011. Using complex resistivity imaging to infer biogeochemical processes associated with bioremediation of an uranium-contaminated aquifer. J. Geophys. Res. 116, G03001. http://dx.doi.org/10.1029/2010JG001591.

Foufoula-Georgiou, E., Kumar, P., 1994. Wavelets in Geophysics. Academic Press, San Diego, CA.

Frei, S., Knorr, K.H., Peiffer, S., Fleckenstein, J.H., 2012. Surface micro-topography causes hot spots of biogeochemical activity in wetland systems: a virtual modeling experiment. J. Geophys. Res. Biogeosci. 117 http://dx.doi.org/10.1029/ 2012JG002012.

Giesemann, A., Jaeger, H.-J., Norman, A.L., Krouse, H.R., Brand, W.A., 1994. Online sulfur-isotope determination using an elemental analyzer coupled to a mass spectrometer. Anal. Chem. 66, 2816–2819. http://dx.doi.org/10.1021/ ac00090a005.

Grinsted, A., Moore, J.C., Jevrejeva, S., 2004. Application of the cross wavelet transform and wavelet coherence to geophysical time series. Nonlinear Process. Geophys. http://dx.doi.org/10.5194/npg-11-561-2004.

Groffman, P.M., Butterbach-Bahl, K., Fulweiler, R.W., Gold, A.J., Morse, J.L., Stander, E.K., Tague, C., Tonitto, C., Vidon, P., 2009. Challenges to incorporating spatially and temporally explicit phenomena (hotspots and hot moments) in denitrification models. Biogeochemistry 93, 49–77. http://dx.doi.org/10.1007/ s10533-008-9277-5.

Guan, K., Thompson, S.E., Harman, C.J., Basu, N.B., Rao, P.S.C., Sivapalan, M., Packman, A.I., Kalita, P.K., 2011. Spatiotemporal scaling of hydrological and agrochemical export dynamics in a tile-drained Midwestern watershed. Water Resour. Res. 47 http://dx.doi.org/10.1029/2010WR009997.

Hansen, D.J., McGuire, J.T., Mohanty, B.P., 2011. Enhanced biogeochemical cycling and subsequent reduction of hydraulic conductivity associated with soil-layer interfaces in the vadose zone. J. Environ. Qual. 40, 1941–1954. http:// dx.doi.org/10.2134/jeq2011.0112.

Harms, T.K., Grimm, N.B., 2008. Hot spots and hot moments of carbon and nitrogen dynamics in a semiarid riparian zone. J. Geophys. Res. 113, G01020. http:// dx.doi.org/10.1029/2007JG000588.

Henderson, R.D., Day-Lewis, F.D., Harvey, C.F., 2009. Investigation of aquifer-estuary interaction using wavelet analysis of fiber-optic temperature data. Geophys. Res. Lett. 36, L06403. http://dx.doi.org/10.1029/2008GL036926.

Hoerling, M., Eischeid, J., Kumar, A., Leung, R., Mariotti, A., Mo, K., Schubert, S., Seager, R., 2014. Causes and predictability of the 2012 Great Plains drought. Bull. Am. Meteorol. Soc. 95, 269–282. http://dx.doi.org/10.1175/BAMS-D-13-00055.1.

Hurley, J.P., Cowell, S.E., Shafer, M.M., Hughes, P.E., 1998. Tributary loading of mercury to Lake Michigan: importance of seasonal events and phase partitioning. Sci. Total Environ. 213, 129–137. http://dx.doi.org/10.1016/S0048- 9697(98)00084-9.

Janicke, H., Bottinger, M., Mikolajewicz, U., Scheuermann, G., 2009. Visual explo- € ration of climate variability changes using wavelet analysis. IEEE Trans. Vis. Comput. Graph 15, 1375–1382. http://dx.doi.org/10.1109/TVCG.2009.197.

Janot, N., Lezama Pacheco, J.S., Pham, D.Q., O'Brien, T.M., Hausladen, D., Noel, V., € Lallier, F., Maher, K., Fendorf, S., Williams, K.H., Long, P.E., Bargar, J.R., 2016. Physico-chemical heterogeneity of organic-rich sediments in the Rifle Aquifer, CO: impact on uranium biogeochemistry. Environ. Sci. Technol. 50, 46–53. http://dx.doi.org/10.1021/acs.est.5b03208.

Kumar, P., Ruddell, B.L., 2010. Information Driven Ecohydrologic Self-organization 2085e2096. Labat, D., 2005. Recent advances in wavelet

analyses: Part 1. A review of concepts. J. Hydrol. 314, 275–288. http://dx.doi.org/10.1016/j.jhydrol.2005.04.003.

Labat, D., Ababou, R., Mangin, A., 2000. Rainfall-runoff relations for karstic springs. Part II: continuous wavelet and discrete orthogonal multiresolution analyses. J. Hydrol. 238, 149–178. http://dx.doi.org/10.1016/S0022-1694(00)00322-X.

Lair, G.J., Zehetner, F., Fiebig, M., Gerzabek, M.H., van Gestel, C.A.M., Hein, T., Hohensinner, S., Hsu, P., Jones, K.C., Jordan, G., Koelmans, A.A., Poot, A., Slijkerman, D.M.E., Totsche, K.U., Bondar-Kunze, E., Barth, J.A.C., 2009. How do long-term development and periodical changes of river-floodplain systems affect the fate of contaminants? Results from European rivers. Environ. Pollut. 157, 3336–3346. http://dx.doi.org/10.1016/j.envpol.2009.06.004.

Lau, K.-M., Weng, H., 1995. Climate signal detection using wavelet transform: how to make a time series sing. Bull. Am. Meteorol. Soc. http://dx.doi.org/10.1175/ 1520-0477(1995)0762.0.CO;2.

Li, W., 1990. Mutual information versus correlation functions. J. Stat. Phys. 60, 823–837. http://dx.doi.org/10.1007/BF01025996.

Liu, C., Shang, J., Shan, H., Zachara, J.M., 2014. Effect of subgrid heterogeneity on scaling geochemical and biogeochemical reactions: a case of U(VI) desorption. Environ. Sci. Technol. 48, 1745–1752. http://dx.doi.org/10.1021/es404224j.

Liu, X., 2013. Coupled Biogeochemical Cycles in Riparian Zones with Contrasting Hydrogeomorphic Characteristics in the US Midwest. Indiana University.

Long, P., 2009. Rifle Integrated Field Research Challenge Site. Quarterly Report, Fiscal Year 2009, 2nd and 3rd Quarters.

Maes, F., Collignon, A., Vandermeulen, D., Marchal, G., Suetens, P., 1997. Multimodality image registration by maximization of mutual information. IEEE Trans. Med. Imaging 16, 187–198. http://dx.doi.org/10.1109/42.563664.

Maraun, D., Kurths, J., 2004. Cross wavelet analysis: significance testing and pitfalls. Nonlinear Process. Geophys. http://dx.doi.org/10.5194/npg-11-505-2004.

McClain, M.E., Boyer, E.W., Dent, C.L., Gergel, S.E., Grimm, N.B., Groffman, P.M., Hart, S.C., Harvey, J.W., Johnston, C.A., Mayorga, E., McDowell, W.H., Pinay, G., 2003. Biogeochemical hot spots and hot moments at the interface of terrestrial and aquatic ecosystems. Ecosystems. http://dx.doi.org/10.1007/ s10021-003- 0161-9.

McGuire, J.T., Smith, E.W., Long, D.T., Hyndman, D.W., Haack, S.K., Klug, M.J., Velbel, M.A., 2000. Temporal variations in parameters reflecting terminalelectron-accepting processes in an aquifer contaminated with waste

fuel and chlorinated solvents. Chem. Geol. 471–485. http://dx.doi.org/10.1016/S0009- 2541(00)00223-0.

Palta, M.M., Ehrenfeld, J.G., Groffman, P.M., 2014. “Hotspots” and “hot moments” of denitrification in urban brownfield wetlands. Ecosystems 17, 1121–1137. http:// dx.doi.org/10.1007/s10021-014-9778-0.

Pinay, G., Clement, J.C., Naiman, R.J., 2002. Basic principles and ecological conse- quences of changing water regimes on nitrogen cycling in fluvial systems. Environ. Manag. 30, 481–491. http://dx.doi.org/10.1007/s00267-002-2736-1.

Pluim, J.P.W., Maintz, J.B.A., Viergever, M.A., 2003. Mutual-information-based registration of medical images: a survey. IEEE Trans. Med. Imaging 22, 986–1004. http://dx.doi.org/10.1109/TMI.2003.815867.

Qafoku, N.P., Gartman, B.N., Kukkadapu, R.K., Arey, B.W., Williams, K.H., Mouser, P.J., Heald, S.M., Bargar, J.R., Janot, N., Yabusaki, S., Long, P.E., 2014. Geochemical and mineralogical investigation of uranium in multi-element contaminated, organic-rich subsurface sediment. Appl. Geochem. 42, 77–85. http://dx.doi.org/ 10.1016/j.apgeochem.2013.12.001.

Qafoku, N.P., Kukkadapu, R.K., McKinley, J.P., Arey, B.W., Kelly, S.D., Wang, C., Resch, C.T., Long, P.E., 2009. Uranium in framboidal pyrite from a naturally bioreduced alluvial sediment. Environ. Sci. Technol. 43, 8528–8534. http:// dx.doi.org/10.1021/es9017333.

Quiroz, R., Yarleque, C., Posadas, A., Mares, V., Immerzeel, W.W., 2011. Improving daily rainfall estimation from NDVI using a wavelet transform. Environ. Model. Softw. 26, 201–209. http://dx.doi.org/10.1016/j.envsoft.2010.07.006.

Salehikhoo, F., Li, L., 2015. The role of magnesite spatial distribution patterns in determining dissolution rates: when do they matter? Geochim. Cosmochim. Acta 155, 107–121. http://dx.doi.org/10.1016/j.gca.2015.01.035.

Sassen, D.S., Hubbard, S.S., Bea, S.A., Chen, J., Spycher, N., Denham, M.E., 2012. Reactive facies: an approach for parameterizing field-scale reactive transport models using geophysical methods. Water Resour. Res. 48 http://dx.doi.org/ 10.1029/2011WR011047 n/aen/a.

Schirmer, M., Luster, J., Linde, N., Perona, P., Mitchell, E.A.D., Barry, D.A., Hollender, J., Cirpka, O.A., Schneider, P., Vogt, T., Radny, D., Durisch-Kaiser, E., 2014. Morphological, hydrological, biogeochemical and ecological changes and challenges in river restoration e the Thur River case study. Hydrol. Earth Syst. Sci. 18, 2449–2462. http://dx.doi.org/10.5194/hess-18-2449-2014.

Scholl, M.A., Cozzarelli, I.M., Christenson, S.C., 2006. Recharge processes drive sulfate reduction in an alluvial aquifer contaminated with landfill leachate. J. Contam. Hydrol. 86, 239–261. http://dx.doi.org/10.1016/j.jconhyd.2006.03.005.

Shannon, C.E., 1948. A mathematical theory of communication. Bell Syst. Tech. J. 27, 379–423. http://dx.doi.org/10.1145/584091.584093.

Singh, V.P., 2011. Hydrologic synthesis using entropy theory: review. J. Hydrol. Eng. 16, 421–433. http://dx.doi.org/10.1061/(ASCE)HE.1943-5584.0000332.

Singh, V.P., 1997. The use of entropy in hydrology and water resources. Hydrol. Process. 11, 587–626.

Starck, J., Murtagh, F., Gastaud, R., 1998. A new entropy measure based on the wavelet transform and noise modeling. IEEE Trans. Circuits 45, 1118–1124.

Steuer, R., Kurths, J., Daub, C.O., Weise, J., Selbig, J., 2002. The mutual information: detecting and evaluating dependencies between variables. Bioinformatics 18 (Suppl. 2), S231–S240. http://dx.doi.org/10.1093/bioinformatics/18.suppl_2.S231.

Strehl, A., Ghosh, J., Mooney, R., 2000. Impact of similarity measures on web-page clustering, in: workshop on artificial intelligence for web search (AAAI 2000). pp. 58–64.

Torrence, C., Compo, G.P., 1998. A practical guide to wavelet analysis. Bull. Am. Meteorol. Soc. 79, 61–78 doi:NA.

U.S. Department of Energy, 2012. Groundwater Compliance Action Plan for the Old Rifle, Colorado, UMTRCA Title I Processing Site.

U.S. Department of Energy, 1999. Final Site Observational Work Plan for the UMTRA Project Old Rifle Site. Grand Junction, CO.

Vazquez, E., Amalfitano, S., Fazi, S., Butturini, A., 2010. Dissolved organic matter composition in a fragmented Mediterranean fluvial system under severe drought conditions. Biogeochemistry 102, 59–72. http://dx.doi.org/10.1007/ s10533-010-9421-x.

Vidon, P., Allan, C., Burns, D., Duval, T.P., Gurwick, N., Inamdar, S., Lowrance, R., Okay, J., Scott, D., Sebestyen, S., 2010. Hot spots and hot moments in riparian zones: potential for improved water quality management. J. Am. Water Resour. Assoc. 46, 278–298.

Vrionis, H.A., Anderson, R.T., Ortiz-Bernad, I., O'Neill, K.R., Resch, C.T., Peacock, A.D., Dayvault, R., White, D.C., Long, P.E., Lovley, D.R., 2005. Microbiological and geochemical heterogeneity in an in situ uranium bioremediation field site. Appl. Environ. Microbiol. 71, 6308–6318. http://dx.doi.org/10.1128/AEM.71.10.6308- 6318.2005.

Wainwright, H.M., Orozco, A.F., Bücker, M., Dafflon, B., Chen, J., Hubbard, S.S., Williams, K.H., 2015. Hierarchical Bayesian method for mapping biogeochemical hot spots using induced polarization imaging. Water Resour. Res. http:// dx.doi.org/10.1002/2015WR017763 n/aen/a.

Williams, K.H., Long, P.E., Davis, J.A., Wilkins, M.J., N'Guessan, A.L., Steefel, C.I., Yang, L., Newcomer, D., Spane, F.A., Kerkhof, L.J., McGuinness, L., Dayvault, R., Lovley, D.R., 2011. Acetate availability and its influence on sustainable bioremediation of uranium-contaminated groundwater. Geomicrobiol. J. 28, 519–539. http://dx.doi.org/10.1080/01490451.2010.520074.

Yabusaki, S.B., Fang, Y., Williams, K.H., Murray, C.J., Ward, A.L., Dayvault, R.D., Waichler, S.R., Newcomer, D.R., Spane, F.A., Long, P.E., 2011. Variably saturated flow and multicomponent biogeochemical reactive transport modeling of a uranium bioremediation field experiment. J. Contam. Hydrol. 126, 271–290. http://dx.doi.org/10.1016/j.jconhyd.2011.09.002.

Zhang, Q., Liu, C., Xu, C., Xu, Y., Jiang, T., 2006. Observed trends of annual maximum water level and streamflow during past 130 years in the Yangtze River basin, China. J. Hydrol. 324, 255–265. http://dx.doi.org/10.1016/j.jhydrol.2005.09.023.

Zhu, Q., Schmidt, J.P., Bryant, R.B., 2012. Hot moments and hot spots of nutrient losses from a mixed land use watershed. J. Hydrol. 414–415, 393e404. http:// dx.doi.org/10.1016/j.jhydrol.2011.11.011.